

Use of Silicon Photomultipliers in ZnS:⁶LiF scintillation neutron detectors: signal extraction in presence of high dark count rates

A. Stoykov, J.-B. Mosset, U. Greuter, M. Hildebrandt, N. Schlumpf

Paul Scherrer Institut, CH-5232 Villigen PSI, Switzerland

We report on the possibility of using Silicon Photomultipliers (SiPMs) to detect the scintillation light from neutron conversion in ZnS:⁶LiF scintillators. The light is collected by wavelength-shifting fibers and adapted to the sensitivity range of the SiPMs. The difficulty of extracting neutron signals in presence of high dark count rates of the SiPMs is addressed by applying a dedicated processing algorithm to analyze the temporal distribution of the SiPM pulses. With a single-channel prototype detection unit we demonstrate a very good neutron signal extraction at SiPM dark count rates of about 1 MHz.

Keywords: SiPM, MPPC, neutron detector, ZnS:LiF, WLS fiber

1 Introduction

The current approaches [1, 2, 3, 4] for large-area multi-channel detectors for thermal neutrons which are based on the scintillation process in ZnS:⁶LiF (ZnS:¹⁰B₂O₃) screens use photomultiplier tubes (PMTs) to detect the scintillation light collected through clear or wavelength-shifting (WLS) fibers. Equipping each detection channel with its own single-anode PMT is not realistic due to cost and detector volume considerations. Light-sharing schemes are applied to reduce the total number of PMTs to be built in. Using multi-anode PMTs in combination with WLS fibers individual channel readouts become feasible. Silicon Photomultipliers (SiPMs), being compact and significantly less expensive than PMTs, could turn out to be advantageous if being used in readout schemes utilizing WLS fibers. But, in contrast to PMTs, SiPMs are photosensors with high intrinsic dark count rates and, considering the long emission decay time of the ZnS scintillator where 25 % (60 %) of the photons are emitted within the first 1 μ s (10 μ s) of a neutron scintillation event [5], one has to face the difficulty of separating the signal events from these dark counts. Below we address this issue.

2 Scintillation neutron detector test structure

Figure 1 shows the design details of the single-channel detection unit (see also [6]) used in the current tests. At one side of this unit the four wavelength shifting (WLS) fibers guiding the scintillation light are glued together and connected to one SiPM. On the other side the fibers are cut along the edge of the sandwich and polished. An aluminized Mylar foil serving as specular reflector is glued on these polished fiber ends. The effective channel width is defined by the area covered by the fibers and is about 2.4 mm. The additional space to the total width of 7 mm is used for handling purposes only. The length of the structure is 50 mm.

In a later multi-channel detector this 2.4 mm wide groove/WLS fiber pattern without the additional handling space will be repeated to cover the needed neutron sensitive area. By stacking several detection structure units of this type, one behind each other, the required neutron absorption probability will be achieved. The number of WLS fibers from these stacked structure units bound to one SiPM and their relative structure pitch define the channel width, as well as the amount of the available light per single event detection. If necessary, the channels could be optically separated, e.g. by cutting narrow grooves between them and filling those grooves with a non-transparent material.

3 Photon detection and signal processing

As photon detector a prototype of the 3x3 mm² MPPC S12572-050C from Hamamatsu [10] was used in the test setup. This SiPM shows compared to earlier types a much lower (< 3%) afterpulse probability [11]. The SiPM was operated with a bias voltage of 67.8 V (overvoltage 2.3 V) at 23.5 °C. The dark count rate at these operating conditions is ~ 1 MHz. For further applications most likely the 1x1 mm² version of the SiPM with a considerably lower dark count rate will be chosen. But one should keep in mind that during operation of the detection system the dark count rate might undergo short-term variations caused by variations of the ambient temperature (if not stabilized), and in long-term it might increase due to radiation induced processes. Accordingly, the signal processing scheme has to be designed in order to allow for elimination of dark count rates as high as possible by simultaneously preserving high detection efficiency for the neutron absorption related photon emission.

The implemented signal processing scheme is not following the classical way of integrating over all the collected scintillation photons from a single detection process and performing a pulse shape analysis later on. Instead a fast single photon detection followed by a time domain filtering is implemented. The basic elements of the processing chain for the SiPM signals are presented in Figure 2. It includes a high band-width amplifier, a leading-edge discriminator, a multistage filter, and an event generator unit.

The SiPM signal is amplified and shaped by a wide band-width gain stage; each SiPM pulse corresponds to one primary charge carrier triggering an avalanche breakdown in one (or more than one by optical cross-talk) of the SiPM cells. This signal is fed into a fast leading edge discrimination stage accepting all SiPM pulses generated either by scintillation photons or thermally. Figure 3 shows a scope “screen-shot” (persistence mode) of the amplified SiPM pulses (SA) and the generated discriminator signals (SD). This kind of digitalization allows for a further signal processing scheme being independent of the SiPM type.

The SD pulse sequence is processed by a “single-pulse elimination” filter implementation (see Figure 4). The delay lines are chosen in order to prevent the initiating SD respectively SF(i) pulses to pass the coincidence-AND gates. To pass this type of filtering stage, a pulse at its input has therefore to show up with a preceding pulse (being part of a pulse group) within the time interval defined by the width of the internal gate (retriggerable “mono-flop” type) signal, i.e. single pulses and always the first pulse from a group of consecutive pulses are removed from the SD respectively SF(i) pulse sequence. At the ED(i) outputs the number of remaining events (single pulses and pulse groups built by the retriggerable mono-flops) can be counted. This counting is only done to analyse the

filter performance, e.g. to determine the remaining dark count rate dependence on the number of stages, and is not necessarily to be implemented.

This kind of filter is scalable, i.e. its basic unit stage can be supplemented by any number of the same basic unit. The adjustable parameters of such a filter type are therefore given by the gate width (each stage is individually configurable) and the number of the consecutive filtering stages. When building up multiple filter stages in series two different choices of time constants have to be considered. Choosing the time constant of the following stage to be identical to those of the previous one increases the number of consecutive pulses which have to fulfill the timing criteria by one. Choosing a longer time constant for the following stage allows for gaps up to this longer time constant within the already decimated pulse sequence. As always only the first pulse of a group is removed from the remaining sequence, over several stages a non-linear filter characteristic (punishing early arriving pulses more than later ones) can be achieved. This behavior together with the time-elasticity of the retriggerable mono-flops allows for passing pulse-sequences with quite different distributions (either high rates within a short time slice or somewhat lower rates over longer time periods). The probability of dark counts passing the filter is dominated by the choice of the gate width of the first filter stage and the total number of consecutive stages.

The application of this filter relies on the fact, that the characteristic SD-pulse rate from a real neutron scintillation event is substantially higher compared to that resulting from thermal generation of charge carries inside the SiPM cells (dark counts).

Figure 5 shows an example of a measured SD and SF pulse sequences from the detection of one neutron scintillation event. The first pulse of the SF signal (a subsequence of SD pulses passing the filter) is triggering the event generator (a retriggerable mono-flop with adjustable pulse width) generating an event signal SN. The width of SN signal is set to prevent multiple triggers from the same scintillation event (late after-glow photon elimination).

4 Measurements

In order to be able to test this "dark count suppression" algorithm with real scintillation photons, measurements with alpha and neutron sources were performed.

The ^{241}Am alpha source is a tablet with a diameter of $\varnothing = 25\text{ mm}$ covered with a 0.2 mm thick aluminium plate having a $16 \times 1.6\text{ mm}$ slit serving as a collimator. The source was positioned below the scintillator structure (see Figure 1). The energy of the alpha-particles is $\sim 5.5\text{ MeV}$, their penetration depth into the scintillator is $\sim 20\ \mu\text{m}$. Consequently, the minimum path for the scintillation light from the point of emission to absorption in a WLS fiber is $\sim 130\ \mu\text{m}$. For absolute efficiency measurements the source was calibrated in the following way: a plastic scintillator was mounted onto the photocathode of a photomultiplier tube and the intensity of alpha-particles was measured to be $94 \pm 1\ 1/\text{s}$. The detection threshold was set low enough to ensure that all alpha-events were detected.

Thermalized neutrons were obtained from a $^{241}\text{AmBe}$ source (activity $\sim 2 \cdot 10^4$ neutrons/s) enclosed in a polyethylene moderator. The rate of thermal neutrons detected with our test detector unit was in the order of 1 count per second. As the neutron interactions are distributed more uniformly within the scintillator volume compared to

the alpha-particle interactions close to the surface of the scintillator, the light collection conditions are expected to be more favorable in case of neutrons.

Figure 6 shows distributions of accumulated numbers of SD-pulses corresponding to the detection of alpha-particles and neutrons. The SD-signal count accumulation time was set to the first $10\ \mu\text{s}$ of the detected events. This parameter (number of SD-counts) was obtained using the measuring capabilities of a LeCroy WaveRunner 640Zi DSO. In case of neutron detection the average number of photon counts is somewhat larger; this can be attributed to the more favorable conditions for the scintillation light collection. This fact allows to perform various optimization studies using a simple ^{241}Am alpha-source.

Figure 7 shows the measured detection efficiency for alpha-particles depending on the gate width of the first filter stage at different (fixed) total numbers of filtering stages. Reasonably achievable values for the alpha detection efficiency are found to be in the range of 80 – 90%. Changing the filter parameters in order to achieve higher detection efficiencies will lead to deterioration of its dark count rejection capabilities and is therefore not recommended.

Figure 8 shows the rate of “residual” dark counts at the filter output as a function of the total number N of filtering stages. Each stage is suppressing the dark-count rate ($\sim 1\ \text{MHz}$ at the filter input) by a factor of about 10, so that at $N = 8$ (where we get an alpha particle detection efficiency of $\sim 82\%$) the residual output dark-count rate finally ends up with about $3 \cdot 10^{-3}\ \text{Hz}$.

Summary

The feasibility of using Silicon Photomultipliers for individual channel readout in multi-channel neutron detection systems utilizing $\text{ZnS:}^6\text{LiF}$ scintillation screens is demonstrated. An efficient light collection is achieved by uniformly distributing $\varnothing = 0.25\ \text{mm}$ WLS fibers inside the sensitive absorption volume for each of the readout channels. A signal processing scheme based on the acceptance of all of the SiPM pulses (generated either by scintillation photons or thermally) with a subsequent efficient suppression of the dark counts is presented.

Within a prototype detection unit using a SiPM with dark-count rate of $\sim 1\ \text{MHz}$ unwanted back-ground events can be suppressed down to a level of $3 \cdot 10^{-3}\ \text{Hz}$, and the implemented suppression algorithm allows for a detection efficiency of $\geq 80\%$ for alpha-particles. For neutrons a higher detection efficiency is to be expected due to the larger amount of photons from one single neutron absorption process.

Optimization of the detector performance and the determination of its additional characteristics such as rate capability, gamma sensitivity, and time resolution will be subjects of further investigations and discussed elsewhere.

Acknowledgments

We express our gratitude to Andreas Hofer (Detector Group of the Laboratory for Particle Physics) for designing and building our prototype detection units.

References

- [1] N.J. Rhodes et al., Nucl. Instr. and Meth. A 392 (1997) 315.
- [2] K. Sakasai et al., Nucl. Instr. and Meth. A 600 (2009) 157.
- [3] T. Nakamura et al., Nucl. Instr. and Meth. A 686 (2012) 64.
- [4] T. Nakamura et al., Nucl. Instr. and Meth. A 741 (2014) 42.
- [5] E.S. Kuzmin et al., Journal of Neutron Research 10(1) (2002) 31.
- [6] J.-B. Mosset et al., arXiv:1309.6885v1
- [7] <http://www.appscintech.com>
- [8] <http://www.kuraray.co.jp>
- [9] <http://www.eljentechnology.com>
- [10] <http://www.hamamatsu.com>
- [11] K. Sato et al., Nucl. Instr. and Meth. A 732 (2013) 427.

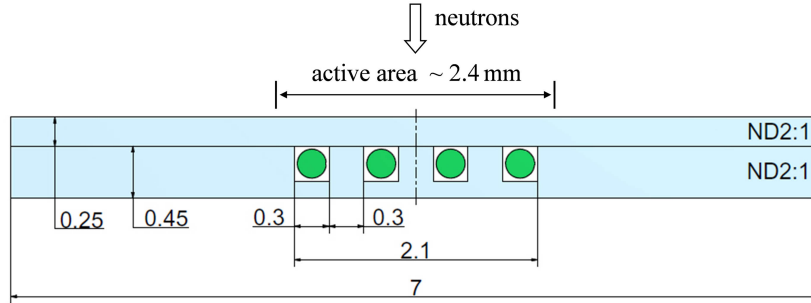


Figure 1: Test scintillator structure used in the present measurements. The scintillators are ND2:1 neutron detection screens from Applied Scintillation Technologies [7], the wavelength-shifting fibers are of type Y11(200)M from Kuraray [8]. The optical epoxy used to glue the fibers into the grooves and the scintillator sheets together is EJ-500 from Eljen [9].

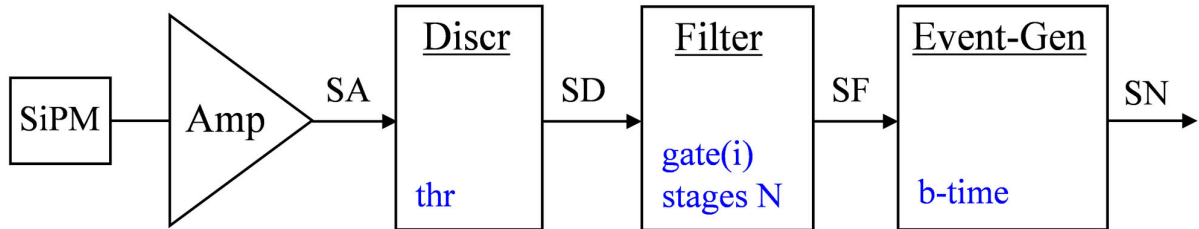


Figure 2: Processing scheme of the SiPM signals: high band-width amplifier, leading-edge discriminator stage, multistage filter, and event generator unit. The tunable parameters are: the discrimination threshold (thr), the number of filter stages (N), the “retriggerable” gate width of each of the filter stages ($gate(i)$), and the duration of the output pulse of the event generator ($b-time$ - “blocking” time) to account for the after-glow photons from the scintillation processes.

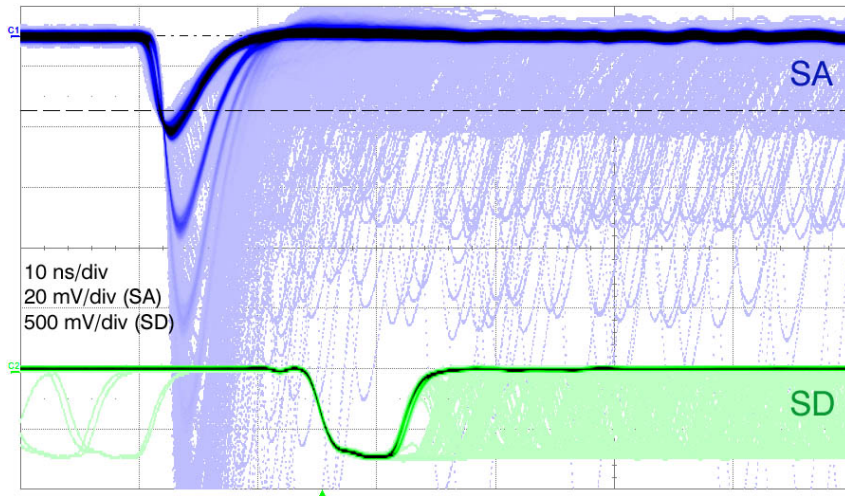


Figure 3: Conversion of the amplified and shaped SiPM analog signals (SA) into standard digital signals (SD) by a fast leading edge discrimination stage.

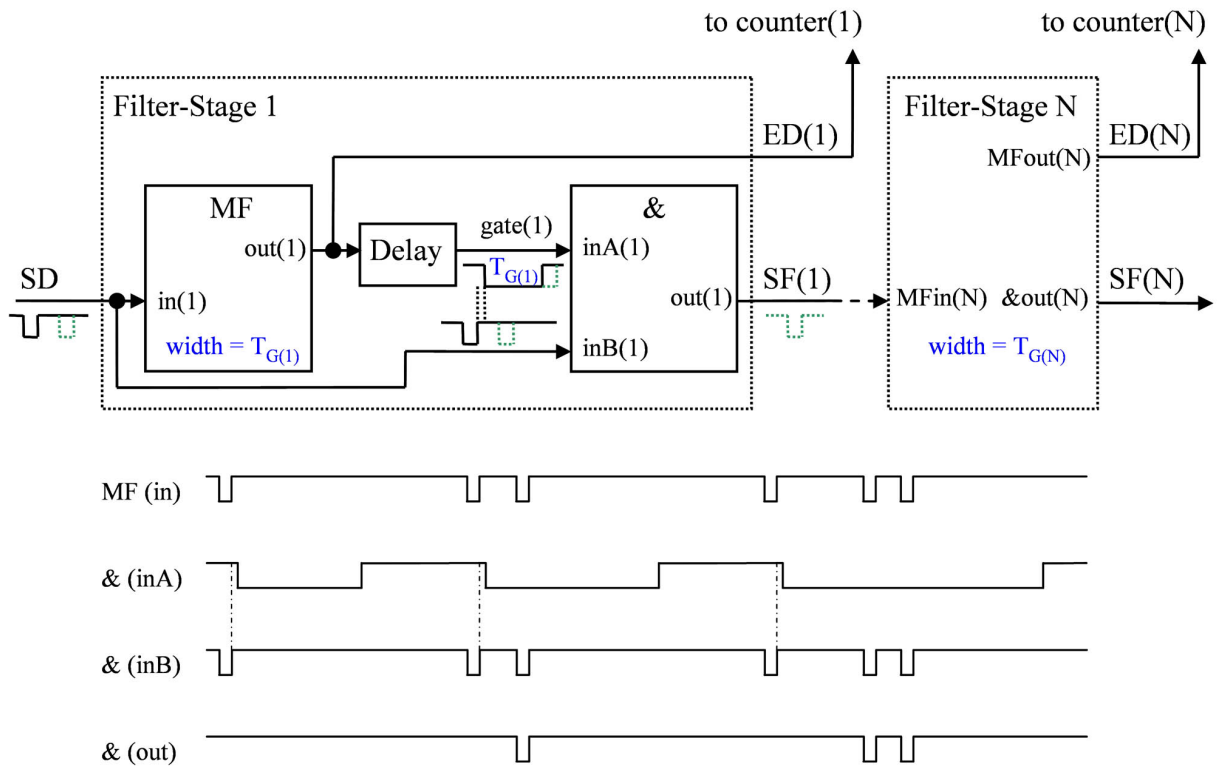


Figure 4: Block diagram (top) of a “single pulse elimination” multistage filter: MF - retriggerable mono-flop, & - coincidence logic. The filter performs a consecutive delayed self-coincidence signal processing on the input SD-pulse sequence. The ED(i) outputs enable to measure the remaining event rate. The timing diagram (bottom) illustrates the passing of pulses through a filtering stage. For clarity the internal delays of “MF” and “&” units are assumed to be zero. The active state is low due to the standard NIM-logic used.

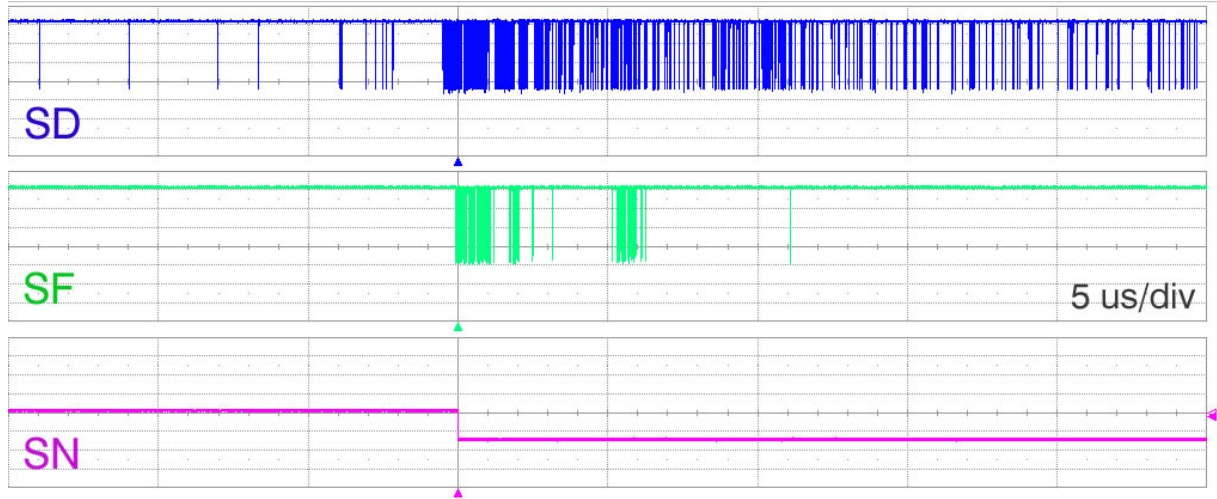


Figure 5: Detection of a neutron event: initial SD pulse sequence and the subsequence of the SD-pulses passing the filter stages (SF-signal). The first pulse of the SF-sequence is generating the leading edge of an event signal (SN). The width of the SN-signal (retriggerable “mono-flop” type) is $100 \mu\text{s}$.

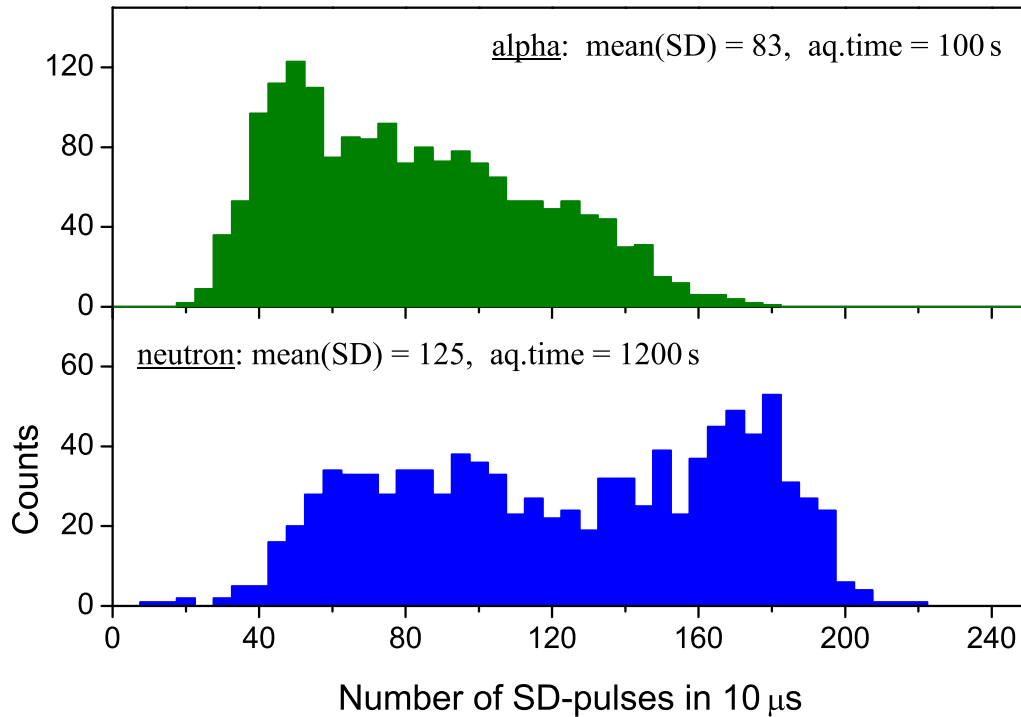


Figure 6: Distribution of the accumulated numbers of SD-counts for the detection of alpha-particles and thermalized neutrons within the first $10 \mu\text{s}$ of the corresponding events. In both cases no collimators were used, accordingly some of the detected events might come from interactions outside the region of optimum light collection covered by the WLS fibers.

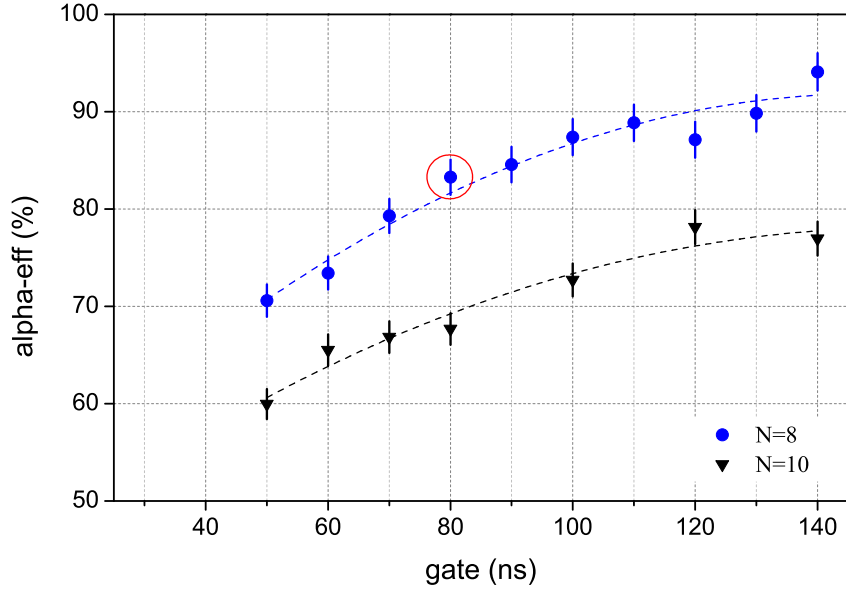


Figure 7: Alpha-particle detection efficiency as a function of the gate width of the first filter stage (all other filter gates are set to 200 ns). The total number of filter stages is fixed ($N=8, 10$). The collimating slit of the alpha-source is oriented along the axis of the scintillator structure. The selected filter setting is indicated by a red circle. The dashed lines are shown to guide the eye.

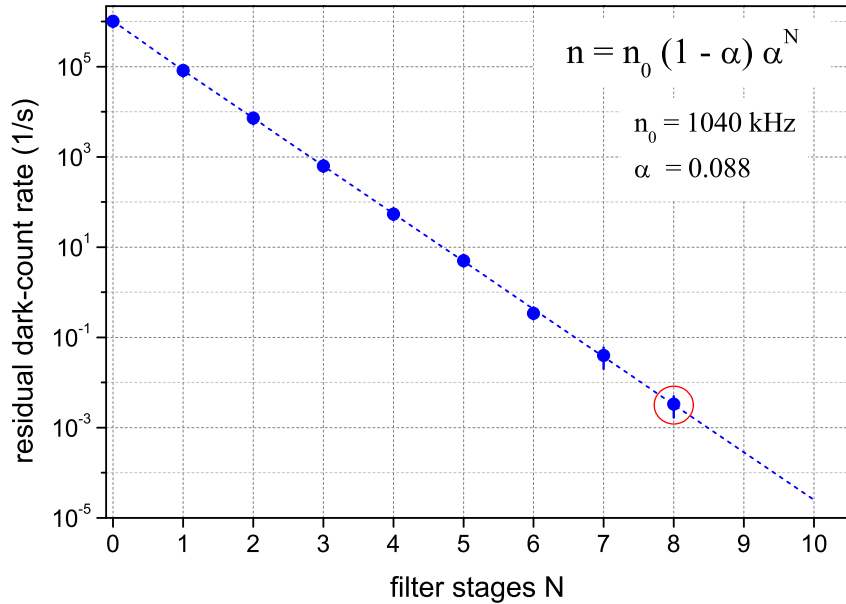


Figure 8: Residual dark-count rate (n) at the filter output as a function of the number of filtering stages (N). Dark-count bunches (groups) with temporal distances between individual pulses of $\leq \text{gate}(i)$ width are just counted as one single pulse. The gate-widths are fixed to: $\text{gate}(1) = 80$ ns, $\text{gate}(i) = 200$ ns. The dashed line is just given to guide the eye: starting from $N=1$ it corresponds to an empirical dependence $n(N)$ as presented in the plot. The point at $N=0$ denotes the input dark count rate of $n_0 = 1040$ kHz.